

Microstructural evolution and growth velocity-undercooling relationships in the systems Cu, Cu-O and Cu-Sn at high undercooling

S. E. BATTERSBY*, R. F. COCHRANE, A. M. MULLIS[‡]
Department of Materials, University of Leeds, Leeds LS2 9JT, UK
E-mail: met6am@sun.leeds.ac.uk

A melt encasement (fluxing) technique has been used to systematically study the velocity-undercooling relationship in samples of Cu and Cu-O and Cu-3 wt% Sn at undercoolings up to 250 K. In pure Cu the solidification velocity increased smoothly with undercooling up to a maximum of 97 m s^{-1} . No evidence of grain refinement was found in any of the as-solidified samples. However, in Cu doped with >200 ppm O we found that samples undercooled by more than 190 K had a grain refined microstructure and that this corresponded with a clear discontinuity in the velocity-undercooling curve. Microstructural evidence in these samples is indicative of dendritic fragmentation having occurred. In Cu-Sn grain refinement was observed at the highest undercoolings (greater than 190 K in Cu-3 wt% Sn) but without the spherical substructure seen to accompany grain refinement in Cu-O alloys. Microstructural analysis using light microscopy, texture analysis and microhardness measurements reveals that recrystallisation accompanies the grain refinement at high undercoolings. Furthermore, at undercoolings between 110 K and 190 K, a high density of subgrains are seen within the microstructure which indicate the occurrence of recovery, a phenomenon previously unreported in samples solidified from highly undercooled melts. © 2000 Kluwer Academic Publishers

1. Introduction

Recalescence velocities as a function of undercooling have been measured for a number of pure metals and alloys growing from their undercooled melts, including Ni [1, 2], Ni-Si [3], Ni-Cu [4], Ge [5, 6], Ge-Sn [7] and Ge-Fe [8]. Generally, this measurement has been made in conjunction with a detailed analysis of the as-solidified microstructure. Such an analysis reveals that most of the systems studied undergo a spontaneous transition from a coarse columnar to a fine equiaxed grain structure above some well defined undercooling ΔT^* . Moreover, this transition appears to be coincident with a discontinuity in the velocity undercooling curve. Below ΔT^* , growth velocity, V , can be adequately represented by current dendritic growth models, with $V \propto \Delta T^\beta$, where $\beta \approx 2.5$. Above ΔT^* , the velocity-undercooling relationship has generally been found to be approximately linear [1, 8], or possibly constant [2].

A number of alloy systems have been reported to show a yet more complex behaviour, in which an equiaxed grain structure at low undercooling gives way to a columnar grain structure as the undercooling is increased. In most of these systems a second region of equiaxed growth appears to occur at yet higher undercooling. It is not clear whether the mechanism for

grain refinement at high undercooling is the same as that operating at low undercooling. Such grain refined microstructures have been observed by Jones and Weston [9] in Cu doped with small quantities of oxygen. At undercoolings below 50 K they found a mixed structure comprising both fine equiaxed and coarser columnar grains, with the proportion of equiaxed grains increasing with undercooling. For $50 \text{ K} < \Delta T < 100 \text{ K}$ they found that the structure was fully equiaxed giving way to a fully columnar structure above 100 K. Mixed grain structures have also been reported in Ni containing oxygen at levels between 0.01 and 0.06 at.% [10] although for oxygen concentrations below 0.01 at.% the grain structure remained columnar at all undercoolings below ΔT^* .

Oxygen is not the only solute which has been reported to give rise to grain refinement at low undercooling. Southin and Weston [11] have found that the addition of sulphur at low concentrations can lead to grain refinement in Cu and that, as for oxygen, a minimum concentration, 0.018 at.%, seems to be required to trigger the effect. The effect has also been observed in some simple binary alloys, such as Ni-Cu [12, 13] and Cu-Sn [14]. In the case of Ni-10 at.% Cu alloys fully equiaxed structures occur for $\Delta T < 60 \text{ K}$ and $\Delta T > 160 \text{ K}$.

* Present Address: British Aerospace plc., Sowerby Research Centre, PO Box 5, Filton, Bristol BS12 7QW.

[‡] Author to whom all correspondence should be addressed.

The origin of spontaneous grain refinement has been controversial since its discovery by Walker [15] in 1959 and a number of mechanisms have been proposed to account for the effect. These include, cavitation in the melt [16], fluid flow effects [17], recrystallisation, dendrite remelting [18] and the development of growth instabilities [19].

Recrystallisation, either during or immediately after solidification, has been observed in rapidly solidified alloys and is a possible mechanism for grain refinement. The driving force for this might be stored energy, due to an increase in defect density as the growth velocity increases, or crystallographic misorientation due to shrinkage induced flow [11]. This model appeared to be supported by measurements made by Ovsienko *et al.* [20] showing that residual microstress in the solid decreases abruptly above ΔT^* . However, Cochrane and Herlach [21] have demonstrated that in drop-tube processed Cu-Ni alloys, if the heat extraction rate is sufficiently high, recrystallisation can be inhibited even in grain refined samples.

Schwarz *et al.* [18] have proposed a surface energy driven fragmentation model to account for grain refinement. Within their model, grain refinement occurs if the local duration of interdendritic solidification, Δt_{pl} , exceeds a time characteristic of dendritic break-up, Δt_{bu} , due to surface area minimisation. As such, their model is dependent both on the undercooling and macroscopic heat extraction rate, an idea which seems to be supported by a parallel study of the alloy $Ti_{63}Nb_{37}$ using both levitation melting and drop-tube techniques [22]. However, as in this model, grain refinement necessarily occurs post-recalescence, the model does not provide an explanation for the change in the velocity-undercooling relationship that accompanies the onset of grain refinement.

Mullis and Cochrane have published an alternative fragmentation model based on a stability analysis of the growth of perturbations to the velocity of the growing tip. Such growth instabilities may occur at both high and low undercooling and their location as a function of ΔT and alloy concentration shows good quantitative agreement with the onset of spontaneous grain refinement [19, 23]. Recently, we have proposed [24] that such an instability may lead to repeated multiple tip splitting, giving rise to a very fine dendritic structure which would undergo rapid remelting to give the observed equiaxed structure seen in grain refined materials. As in this model remelting is related to a growth instability at the tip, it would provide a natural explanation for the break in the velocity-undercooling curve which has been observed in many systems to be coincident with ΔT^* . Moreover, this is consistent with recent high speed video images of droplet recalescence [25] which show a distinct change in front morphology above ΔT^* .

Recently Galenko and Danilov [26] have proposed that the break in the velocity-undercooling curve can be attributed to the finite speed of solute diffusion in the bulk liquid ahead of the growing dendrite. In their model the conventional Fickian diffusion equation, which permits an infinite speed of diffusion, is replaced by a hyperbolic equation containing both diffusion-like

and wave-like terms. As the diffusive speed, V_D , is finite there is an abrupt transition to complete solute trapping when the growth velocity exceeds V_D . In contrast, conventional growth models predict a gradual onset of solute trapping. Calculations by Galenko and Danilov indicate that this abrupt transition to solute trapping results in a discontinuity in the velocity-undercooling curve at V_D , and their results are in good agreement with experimental velocity undercooling curves for the Ni-Cu system. However, it is not clear from the model of Galenko and Danilov why such a break in the velocity-undercooling curve should be observed in pure materials [1, 2, 5, 6], where solute effects are absent.

In this paper, we report on recalescence velocity measurements and microstructural analysis that has been performed on highly undercooled copper and dilute binary copper alloys via a melt encasement technique. In particular, two alloy systems have been studied, Cu-O and Cu-3 wt% Sn. Both of these systems show spontaneous grain refinement in that, above a critical undercooling, ΔT^* , there is an abrupt transition from a coarse columnar to a fine grain equiaxed microstructure. However, there are sufficient differences in the microstructural characteristics of the two systems to lead us to believe that different mechanisms may be responsible for the observed grain refinement.

A number of authors have previously studied the undercooling behaviour of Cu and Cu-O alloys. Powell and Hogan [27] used a glass encasement technique to undercool pure Cu and Cu-O alloys with oxygen concentrations of 0.08 wt% and 0.3 wt%, although the maximum undercooling for the higher oxygen concentration was limited to 97 K. In pure Cu they found no evidence of grain refinement up to a maximum undercooling of 208 K. In Cu-0.08 wt% O they observed a transition from a coarse columnar to fine grained equiaxed structure above $\Delta T = 150$ K. Kobayashi and Shingu [28] were similarly unable to observe grain refinement in pure Cu melts with a maximum undercooling of 225 K. Grain refined microstructures were observed in Cu-O alloys containing >300 ppm O. Using a similar technique, Costa Agra Mello and Kiminami [29] observed grain refinement in pure Cu at an undercooling of 271 K, although they did not investigate lower undercoolings to identify the transition temperature between columnar and equiaxed growth.

2. Experimental techniques

Undercooling experiments were performed within a stainless steel vacuum chamber evacuated to a pressure of 5×10^{-5} mbar and backfilled to 500 mbar with N_2 gas. Samples were heated, in fused quartz crucibles, by induction heating of a graphite susceptor contained within an alumina shell. Viewing slots were cut in the susceptor and alumina to allow the sample to be viewed through a window in the chamber. Melt encasement, within a soda lime glass flux, was employed to reduce the number of potential heterogeneous nucleation sites allowing the attainment of high undercoolings. Temperature determination was by

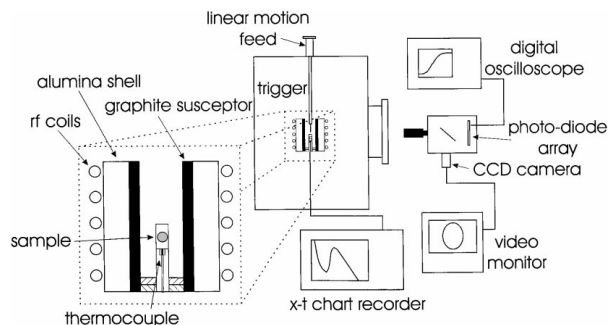


Figure 1 Schematic diagram of fluxing apparatus used for melting and undercooling of Cu, Cu-O and Cu-Sn alloy specimens and the determination of growth velocity-undercooling relationships.

means of a k-type thermocouple positioned beneath the crucible, which had been thinned at the base so reducing the thermal lag between the sample and thermocouple. Cooling curves were obtained with the aid of a chart recorder. A schematic diagram of the experimental apparatus is shown in Fig. 1. By heating the sample to its melting temperature, cooling and repeating this procedure, it was found that melting temperatures were reproducible to within ± 5 K. On heating, the sample and flux were taken to 300 K above the melting temperature to ensure complete melting of the glass, encasement of the sample and the removal of gas bubbles from the flux. The samples were subsequently cooled to a predetermined temperature before nucleation was triggered by touching the sample surface with a thin alumina needle.

The measurement of growth velocities was performed using a 16-element linear photo-diode array, allowing the time taken for the bright recalescence front to move across the relatively dark sample to be measured. Light from the sample was passed through a beam splitter which distributed the light between a CCD camera and the photo-diode array. The CCD camera allows accurate sample positioning and focusing. It was also possible via this arrangement to measure directly the dimension of the sample along the photo-diode axis. A current proportional to the light intensity falling on each photo-diode is produced which was then amplified and recorded. Each of the 16 photo-diodes has an independent, fast settling, low noise, DIFET amplifier with a current to voltage gain of 10^6 V A⁻¹. The signals are then passed, via switching circuitry, to a pair of voltage adders for output. The output signal is displayed as light intensity vs time trace on a digital storage oscilloscope from which the time taken for the solidification front to move through the sample could be measured.

Copper samples, in the size range 3–5 mm and of 99.9999% purity (metals basis), were obtained from ALFA (Johnson Matthey). These samples contain, however, a residual level of oxygen. A number of samples were superheated to 1523 K in the fluxing apparatus and held at this temperature for increasing lengths of time. After solidification, the final oxygen content was determined using a thermal conductivity method and compared to the residual level of oxygen in the as-received samples. From this procedure, we determined

that the oxygen concentration, [O], decreased exponentially with processing time, according to:

$$[\text{O}]/\text{ppm} = 799 \exp\{-0.025t\} \quad (1)$$

with a minimum achievable base level of ≈ 10 ppm. Here we have defined Cu-O alloys as copper containing at least 200 ppm of oxygen after undercooling and oxygen-free copper as containing less than 200 ppm of oxygen, based on the work of previous researchers [28]. The average oxygen concentration of our Cu-O alloy was 600 ppm.

Cu-3 wt% Sn alloy was formed by arc melting under an inert atmosphere to ensure complete mixing of the components. As with Cu, elemental Sn was obtained from ALFA (Johnson Matthey) with a purity of 99.9999% (metals basis). Samples, in the size range 3–5 mm, were subsequently weighed to ensure no mass loss during arc melting.

Microstructural changes as a function of undercooling were initially determined by using a CamScan Series 4 SEM to observe the surface of as-solidified droplets. Further analysis of selected samples was performed by optical microscopy on polished sections using a Nikon Optiphot microscope in differential interference contrast (DIC) mode, samples having been etched in ferric chloride (10 g per litre) to give grain boundary contrast or ammonium persulphate (100 g per litre) to reveal substructure within grains. X-ray pole figure plots were also generated using a Philips APD1700 diffractometer (Cu K α radiation) equipped with a texture stage. Vickers microhardness measurements were made on polished sections of specimens mounted in Bakelite using a Zwick microhardness tester, applying a load of 1000 gf for 20 s.

3. Results

For the three systems studied maximum undercoolings of 250 K (Cu/Cu-O) and 208 K (Cu-3 wt% Sn) were achieved. Recalescence velocities as a function of undercooling for the three systems studied are shown in Fig. 2. For pure Cu and Cu-3 wt% Sn alloy, the experimental points appear to lie on a smooth curve

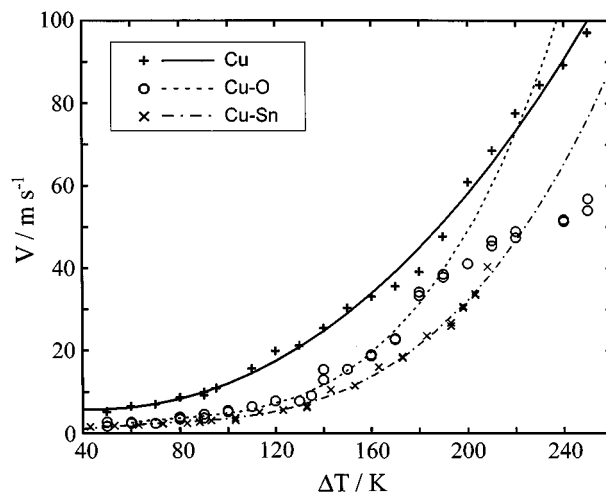


Figure 2 Velocity-undercooling relationships determined for dendritic growth in pure Cu and dilute Cu-O and Cu-Sn alloys.

over the whole undercooling range studied. However, for the Cu-O system there appears to be a distinct break in the curve at $\Delta T \approx 180$ K. Above this undercooling the growth velocity appears to increase linearly with undercooling. As discussed below, this discontinuity in the curve is coincident with the onset of spontaneous grain refinement, an association that has previously been made in a number of other systems [1, 2, 6]. The maximum measured growth velocities were 97 m s^{-1} in copper, 56.8 m s^{-1} in the Cu-O alloy ($\Delta T = 250$ K) and 40.4 m s^{-1} in the Cu-Sn system ($\Delta T = 208$ K).

Samples of oxygen-free copper (<200 ppm oxygen) were selected for microstructural examination at undercoolings ranging from 50–250 K at intervals of approximately 20 K. At all undercoolings the microstructure consisted of coarse grains, the size of which decreased smoothly with increasing undercooling. These results are consistent with the findings of Kobayashi and Shingu [28] who found no evidence of spontaneous grain refinement in Cu melts containing <300 ppm Oxygen (with a maximum undercooling of 225 K) and Costa Agro Mello and Kiminami [29] who observed grain refinement above 270 K, marginally higher than our maximum achievable undercooling.

In contrast, in both alloy systems a number of distinct regions of microstructural development were identified. In Cu-O there were four such regions:

i) **40 K $\leq \Delta T \leq 60$ K.** Fig. 3 shows an example of the microstructure in a sample undercooled by 40 K: the majority of the area of the micrograph is occupied by a single grain. Samples undercooled in the range 40–60 K showed a very large grain size and a very coarse dendritic segregation pattern. The dendritic substructure is not confined to one 'grain' but extends across the one visible grain boundary, suggesting that a significant amount of post-solidification grain coarsening has occurred. Fig. 4 shows a $\{111\}_{\text{Cu}}$ pole figure plot from a Cu-O sample undercooled by 40 K prior to solidification. There are four intense poles present, suggesting that the structure is dominated by a single dendrite grown from the melt, in good agreement with the microstructure shown in Fig. 3 which is dominated by one grain.

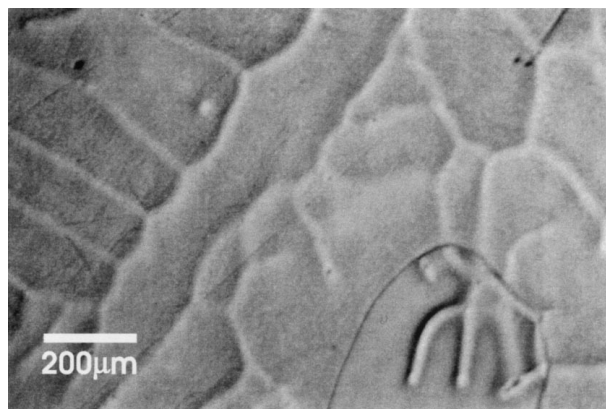


Figure 3 Optical micrograph of Cu-O sample solidified from an undercooling of 40 K. The dendritic substructure can clearly be seen crossing a grain boundary in the lower right hand corner.

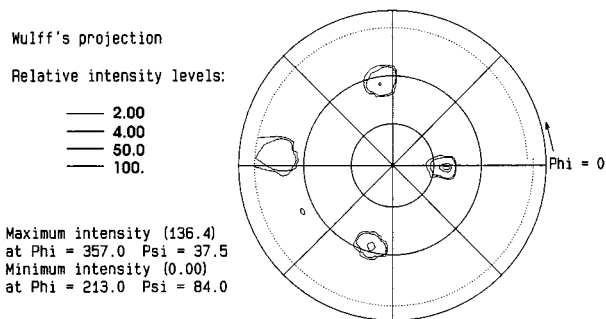


Figure 4 X-ray pole figure plot for $\{111\}_{\text{Cu}}$ taken from the sample shown in Fig. 3.

ii) **70 K $\leq \Delta T \leq 100$ K.** As the undercooling increases in the range 70 K–100 K, a change in structure is observed from dendritic to equiaxed. This can be determined from SEM microscopy of the surface structure (Fig. 5b), removing the need to produce large numbers of polished sections. The microstructure observed in a plane section of the alloy undercooled by 90 K prior to nucleation is shown in Fig. 6. Grain boundaries appear to be decorated by copper oxide particles and a fine interdendritic distribution of either copper oxide or shrinkage pores is present. Within the grains, there are several small spherical elements whose edges and centres have etched strongly. Appreciable grain growth has evidently occurred as the substructure extends across grain boundaries and the grain boundaries themselves are curved which is indicative of grain boundary migration. X-ray pole figures confirmed that these fine grains were randomly oriented. In Fig. 7, a number of poles are observed which are distributed quite randomly across the plot. This would appear to suggest that if a single dendrite dominates the growth at these low undercoolings, this has subsequently fragmented, the fragments acting as nuclei for new grains. During slow cooling, these may coarsen to give the final microstructure observed in Fig. 6.

iii) **110 K $\leq \Delta T \leq 180$ K.** Increasing the undercooling further results in a dendritic surface structure, as observed previously at lower undercoolings but with a finer secondary dendrite arm spacing (Fig. 5c). In this range of undercooling, the grain size was very coarse and optical microscopy (Fig. 8) revealed a well developed dendritic network within each grain. Compared to the coarse, dendritic structure formed at lower undercoolings, the substructure is mostly restricted to one grain. Fig. 8 also clearly shows that there are some very small grains located at the boundaries between some of the larger grains.

iv) **$\Delta T > 180$ K.** At undercoolings greater than 180 K, SEM examination (Fig. 5d) shows that the dendritic surface has been replaced by an equiaxed surface structure which is present in all samples up to the maximum undercooling of 250 K. Fig. 9 reveals that the grain size is comparable to that seen in samples undercooled in the range 70–100 K and again varies considerably throughout the section. Within the grains, the substructure is spherical, the well developed dendrites seen in samples undercooled by 110–180 K being no longer evident. Within some of the spherical segregation

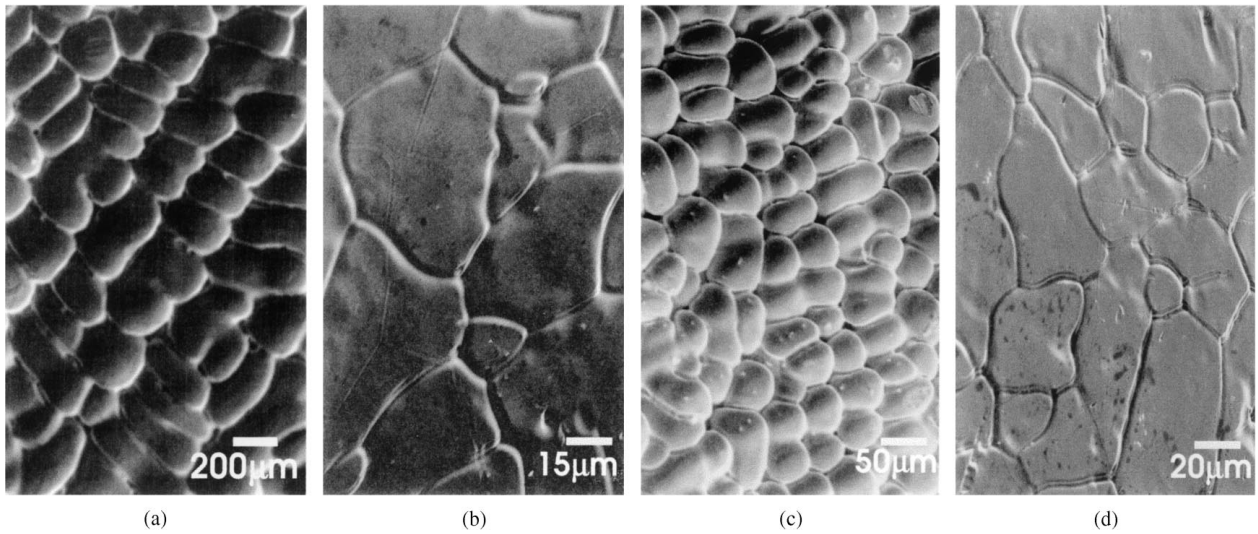


Figure 5 SEM micrographs showing the surface structures of Cu-O specimens solidified from undercoolings of (a) 40 K, (b) 80 K, (c) 160 K and (d) 220 K.

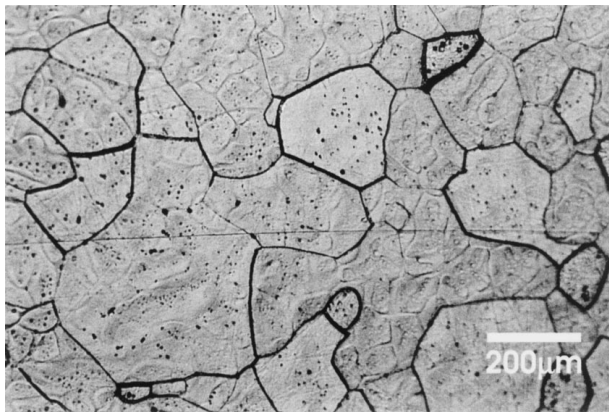


Figure 6 Optical micrograph of Cu-O sample solidified from an undercooling of 90 K.

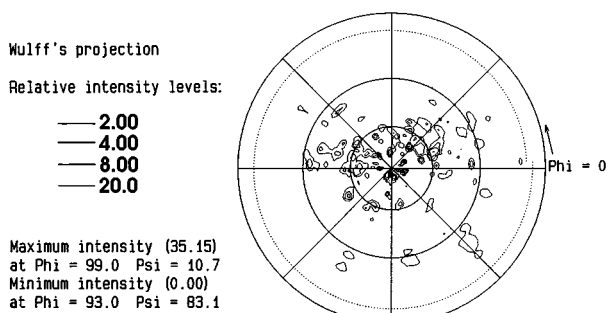


Figure 7 X-ray pole figure plot for $\{111\}_{\text{Cu}}$ taken from the sample shown in Fig. 6.

elements, a small fragment is observed which is cross-shaped or in some cases a small sphere. Another contrasting feature here, as compared with microstructures observed in the other grain refinement regime ($70 \text{ K} < \Delta T < 100 \text{ K}$), is the disappearance of the fine distribution of black copper oxide particles which was very prominent in Fig. 6. However, the shape of the grains and the fact that the substructure is not confined to just one grain suggest that there was some coarsening of grains during cooling in the solid state. X-ray diffractometry of samples (Fig. 10) was consistent with

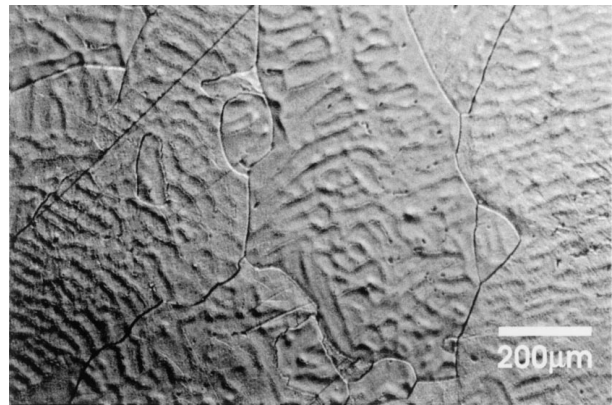


Figure 8 Optical micrograph of Cu-O sample solidified from an undercooling of 160 K.

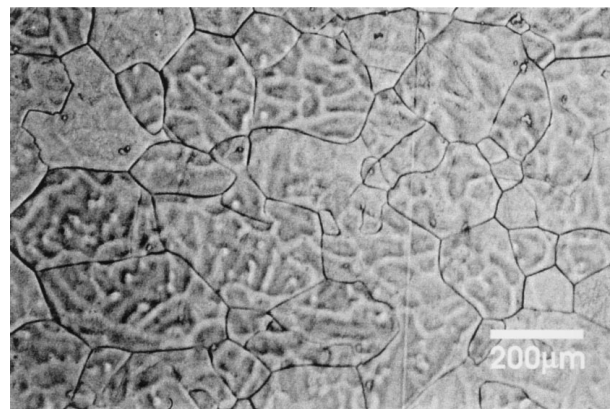


Figure 9 Optical micrograph of Cu-O sample solidified from an undercooling of 250 K.

the equiaxed microstructure observed, the $\{111\}_{\text{Cu}}$ pole figure showing that there are many randomly oriented grains present.

In the Cu-Sn three distinct microstructural regimes were identified:

i) $43 \text{ K} \leq \Delta T \leq 73 \text{ K}$. Fig. 11 shows the microstructure of a sample undercooled by 43 K. It exhibits a

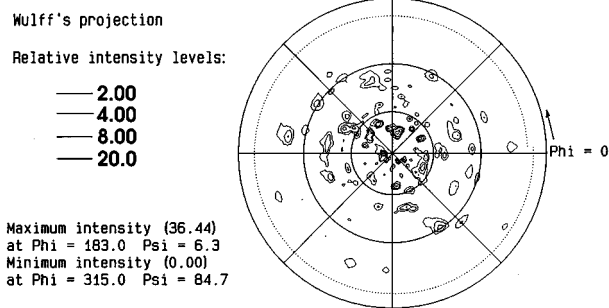


Figure 10 X-ray pole figure plot for $\{111\}_{\text{Cu}}$ taken from the sample shown in Fig. 9.

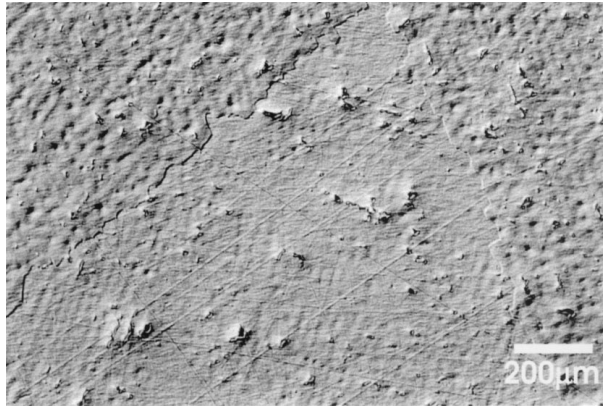


Figure 11 Optical micrograph of Cu-3 wt% Sn sample undercooled by 43 K prior to solidification.

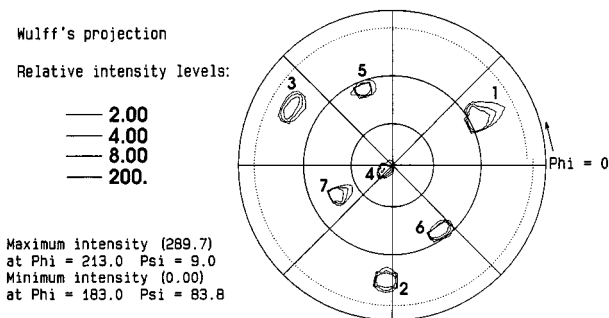


Figure 12 X-ray pole figure plot for $\{111\}_{\text{Cu}}$ from the same sample shown in Fig. 11.

coarse grain size and the combination of etchant and differential interference contrast reveals the substructure which is clearly dendritic but either not fully developed or slightly deformed, with grains that appear to radiate outwards from one point. The grain boundaries here are not straight, in fact they are considerably irregular. X-ray diffractometry gives further information about these microstructures. Fig. 12 shows the pole figure plot obtained for the sample undercooled by 43 K. By measuring the angles between poles, it was determined that this sample has grown as a twinned dendrite. Each of the poles 1–6 has a common angle of either $72^\circ 53'$ or $109^\circ 47'$ with pole 7 and the poles can be grouped into two groups of four by using pole 7 twice, i.e. (1, 2, 3 and 7) and (4, 5, 6 and 7). A twin relationship can be shown to exist between the two grains by rotating the plot to a different orientation with this common pole at the centre.

ii) $73 \text{ K} < \Delta T \leq 193 \text{ K}$. Fig. 13 shows an optical micrograph of a sample undercooled by 123 K prior to nucleation. There are a number of large grains visible containing a very well developed dendritic segregation pattern, the dendrites apparently confined to a single grain. Although there are a number of smaller grains present at the boundaries of the large grains, on the whole, it can be seen that the overall grain size is very coarse and there is no evidence of any breakdown of the dendritic structure. Within this range of undercoolings, as the undercooling increases the grain size decreases slightly but further interesting microstructural features become apparent. Fig. 14 shows the microstructure of a sample undercooled by 183 K. The grain size is quite coarse but within the grains a network of finer grains or subgrains may be clearly seen. Thus, both high angle grain boundaries and low angle boundaries are evident in this micrograph. This effect is uniform across all the grains, i.e. the subgrains are not just seen at the grain boundaries. This strongly suggests that a recovery process has occurred in the solid state following solidification.

iii) $\Delta T > 193 \text{ K}$. At undercoolings greater than 193 K, another type of microstructure was observed. Fig. 15 shows the microstructure of a sample undercooled by 208 K. The grain size is much finer and the segregation pattern seen within the grains is again mostly dendritic, although there seem to be some spherical elements present. The curvature of the grain

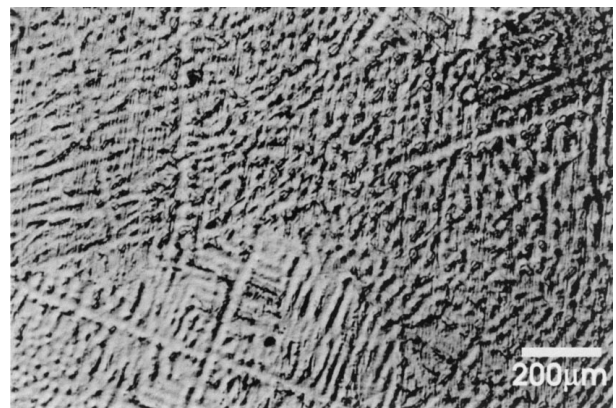


Figure 13 Optical micrograph of a Cu-3 wt% Sn sample undercooled 123 K prior to solidification.

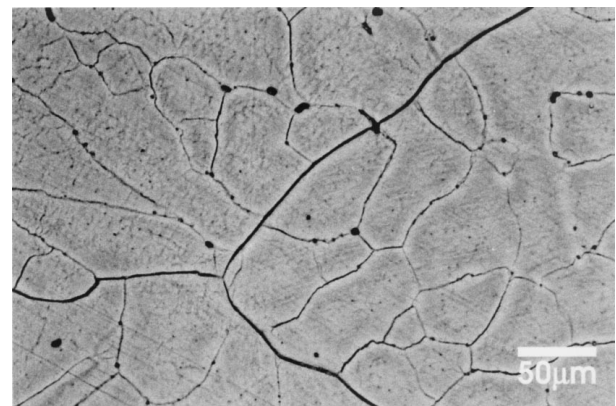


Figure 14 Optical micrograph of a Cu-3 wt% Sn sample undercooled 183 K prior to solidification.

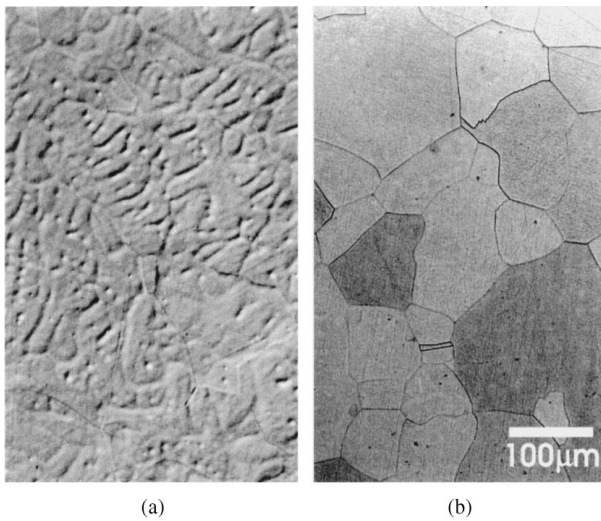


Figure 15 Optical micrograph of a Cu-3 wt% Sn sample undercooled 208 K prior to solidification: (a) etched in ammonium persulphate solution; (b) etched in ferric chloride solution.

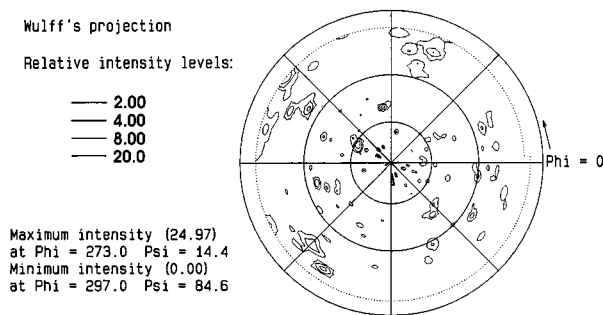


Figure 16 X-ray pole figure plot for $(111)_{\text{Cu}}$ from the same sample shown in Fig. 15.

boundaries indicates that some grain boundary migration has occurred. The subgrains observed in samples undercooled by 183 K and 193 K are absent but there are twins present which are strongly suggestive of recrystallisation. Fig. 16 shows the pole figure plot obtained by x-ray diffractometry for this sample. The distribution of poles is random indicating that a large number of randomly oriented grains are present.

Microhardness measurements were made on samples of Cu-O and Cu-3 wt% Sn solidified at various undercoolings. Results from these measurements are shown in Fig. 17. In Cu-Sn the microhardness increases to a maximum value of 427 kgf mm^{-2} at an undercooling of 183 K and then decreases with further increases in undercooling to 352 kgf mm^{-2} at $\Delta T = 200 \text{ K}$. Such a drop in the microhardness is also indicative of a recrystallization process. In contrast, in Cu-O there is a smooth increase in microhardness with undercooling from 250 kgf mm^{-2} at $\Delta T = 40 \text{ K}$ to 386 kgf mm^{-2} at $\Delta T = 250 \text{ K}$. There is no decrease in microhardness such as would be expected if recrystallisation had occurred. However, there is an apparent change in behaviour in the range $120 \text{ K} < \Delta T < 180 \text{ K}$ which may result from an increase in the matrix solute level due to solute trapping.

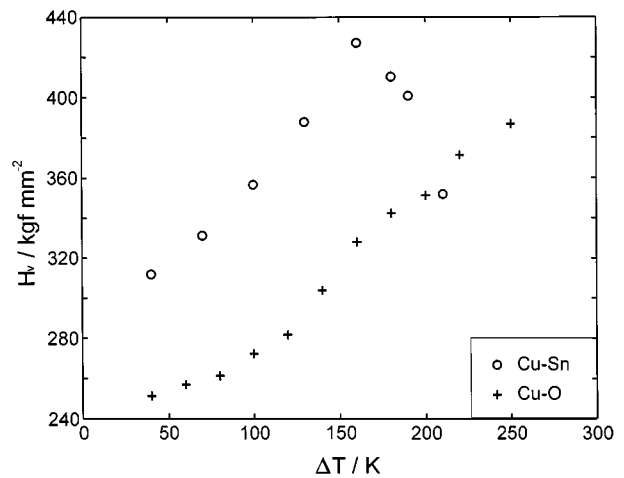


Figure 17 Microhardness vs undercooling results for Cu-3 wt% Sn and Cu-O.

4. Discussion

The presence of a small amount of oxygen in copper samples has been shown to have a profound effect on both the observed microstructures and the growth velocity-undercooling relationship. At oxygen concentrations less than 200 ppm the microstructure remains columnar over the whole range of undercoolings studied but at greater concentrations grain refinement is observed at both low and high undercooling. Grain refinement has been observed in pure copper samples undercooled by 271 K [28] and 320 K [7]. A comprehensive investigation of undercooled Cu-O alloys by Kobayshi and Shingu [28] related the microstructure observed to the oxygen content. Therefore, we believe that grain refinement in pure Cu would have been observed if higher melt undercoolings could have been achieved.

Grain refinement was observed in Cu-O at both low ($70 \text{ K} \leq \Delta T \leq 100 \text{ K}$) and high ($\Delta T > 180 \text{ K}$) undercoolings as an abrupt change in grain size accompanied by a change in segregation pattern from dendritic to spherical. Grain refinement at high undercoolings is accompanied by a deviation in the velocity-undercooling relationship from that predicted by current dendrite growth models (Fig. 2). We suggest, therefore, that grain refinement in Cu-O is caused by dendritic fragmentation. Pole figure plots generated for samples undercooled by 90 K and 250 K confirmed that the pre-existing, highly oriented dendritic structure had broken up, which resulted in a multiplication of grains. This assumption is supported by the observation in Cu-O that the size of spherical elements observed at the centre of grains was comparable to the secondary dendrite arm spacing. Solute trapping may aid these processes as it has been shown here that copper containing less than 200 ppm oxygen did not grain refine at undercoolings up to 250 K. However, the addition of a greater quantity of this strongly partitioning solute resulted in grain refinement at both low and high undercoolings.

At low undercooling there is considerable evidence for grain boundary migration in both non-refined and grain refined structures, the underlying segregation pattern not being consistent with the grain structure. In

the non-refined regime this was apparent from a dendritic network running across grain boundaries, as is clearly the case in Fig. 3, while in grain refined samples some grains contained more than one spherical segregation element. This is consistent with the slow cooling rates typical of fluxing experiments, which would tend to aid grain boundary migration. However, it was apparent that no recrystallisation occurred in these samples. This could be seen microstructurally due to an absence of annealing twins and also in the microhardness measurements where there was a gradual increase in microhardness as a function of undercooling. Consequently we conclude that the line defect density in the as-solidified Cu-O samples at the highest undercoolings is too small to provide the necessary driving force for the recrystallisation process.

In Cu-Sn within the undercooling regime $43 \text{ K} \leq \Delta T \leq 73 \text{ K}$, the coarse grains observed within the microstructure had a twinned relationship. This was confirmed by generating pole figure plots. At low undercoolings, twinned dendrites might give a slight growth advantage over non-twinned dendrites, which disappears at higher undercoolings. Such twinned dendrites have also been observed in DC-cast aluminium alloys [30] where they are responsible for features commonly known as 'feather grains'. The dendritic substructure in these samples was apparently highly deformed: the substructure was poorly developed, it was difficult to identify the dendrite trunks and the secondary dendrite arms appeared bent and fragmented. At these relatively small undercoolings, it may be possible that the dendrites which are formed during recalescence are sufficiently thin to be deformed by fluid flow, which may arise during the growth of undercooled melts due to strong convection or by the volume change which accompanies solidification.

As the undercooling is increased, growth of twin-free dendrites takes place at $\Delta T > 73 \text{ K}$ yielding a substructure of well-developed, columnar dendrites. However, at higher undercoolings, $183 \text{ K} \leq \Delta T \leq 193 \text{ K}$, a change in the grain structure was observed. The coarse columnar grains now contain an array of fine subgrains. The presence of subgrains within a microstructure is an indication that a recovery process has occurred. This deduction is supported by the microhardness data which shows a drop above $\Delta T = 183 \text{ K}$ to levels comparable to those obtained at the lowest undercoolings studied. Recovery would require a driving force, the magnitude of which must increase as the undercooling increases. Unlike recrystallisation, which could be driven by an increased concentration of point or line defects, recovery can only take place in the presence of a high density of dislocations which are probably produced by the dendrite deformation which was observed clearly at lower undercoolings.

The microstructure seen in the most highly undercooled samples revealed a much finer, equiaxed grain structure but with a clearly dendritic segregation pattern. Thus, the refined grain structure observed in highly undercooled Cu-Sn was markedly different to that observed in Cu-O and which has generally been reported in other grain refined alloy systems, the substructure be-

ing dendritic in nature, rather than spherical. Similarly, the surface structure of Cu-3 wt% Sn, undercooled by 208 K, was dendritic, compared to that of grain-refined Cu-O alloys which, at both low and high undercoolings is equiaxed.

Comparing our results for the Cu-Sn system with most other reported cases of spontaneous grain refinement, including our Cu-O alloy, we suggest that there may be at least two distinct mechanisms which can lead to grain refinement. We take grain refinement to be a significant decrease in grain size at a well-defined undercooling together with a transition from a columnar to an equiaxed structure. In most cases previously reported, this is accompanied by a change from a dendritic to spherical segregation pattern and a discontinuity in the velocity-undercooling curve. Evidence for recrystallisation is often found to accompany the transition from a dendritic to spherical segregation pattern in these grain refined materials, although our Cu-O results would indicate that this need not necessarily be the case, there being no evidence of recrystallisation. By contrast, Cu-Sn grain refined samples retain a dendritic substructure despite showing equiaxed grains with a random crystallite orientation. Microstructural and microhardness data suggest that in Cu-Sn grain refinement is a consequence of a recrystallisation process in the solid state. This contrasts with 'conventional' grain refined materials where refinement appears to be the result of dendritic fragmentation during the growth phase.

The processes of dendritic fragmentation and recrystallisation will have different dependencies upon the material parameters of the system being considered. Why recrystallisation should precede fragmentation in CuSn while fragmentation occurs before recrystallisation in CuO is thus not easy to establish. A number of models for grain refinement by fragmentation exist and we discuss below a calculation based on the model of Mullis and Cochrane [19] which is consistent with the experimental results presented. However, to provide a definitive answer it is also necessary to estimate the undercooling at which grain refinement by recrystallisation occurs, a calculation that is far from trivial. The principal driving force for recrystallisation in CuSn is at present unknown, it being unclear whether this is due to an increase in the density of point or line defects. Even if the mechanism can be elucidated, there is no well-defined route for estimating the density of either defect type as a function of recalescence velocity. Moreover, the mechanical properties of Cu and its dilute alloys are so poorly known in the vicinity of the solidus temperature that it may not be possible to estimate the likelihood of recrystallisation, even if the defect density were known.

The Mullis and Cochrane [19] model for grain refinement by dendritic fragmentation is based on a stability analysis of the growth of perturbations to the velocity of the growing tip. The rationale behind the analysis is as follows. The growth velocity is considered to be determined by the difference between the interface temperature and the far field temperature, that is by the thermal undercooling. Curvature, constitutional and kinetic effects are treated as velocity and radius dependant

depressions to the local interface temperature. A velocity perturbation will thus perturb the interface temperature via the actions of the curvature, kinetic and constitutional components of the undercooling. However, this perturbation to the interface temperature will itself result in a velocity perturbation $\delta V'$. Should $|\delta V'| > |\delta V|$ it is presumed that the resultant perturbation grows in a manner which is unchecked, leading to grain refinement. Performing the calculation for Cu-O we obtain a value for the upper grain refinement temperature, ΔT_2^* , of 183 K at an oxygen concentration of 200 ppm rising to 190 K at an oxygen concentration of 600 ppm, in good agreement with the experimental result obtained here. In contrast, for Cu-Sn we calculated the undercooling for the onset of grain refinement by dendritic fragmentation as 207 K, above the observed onset of recrystallisation at 193 K and only 2 K below the maximum undercooling achieved. This result is therefore consistent with our observation that Cu-3 wt% Sn grain refines by recrystallisation.

It thus appears that there are two, independent mechanisms whereby grain refinement can occur at high undercoolings—dendrite fragmentation and recrystallisation—and that each of these processes has a critical undercooling. In some systems (e.g. Fe-Ni and Cu-Ni) these are coincident whereas in others the recrystallisation mechanism precedes fragmentation (e.g. Cu-Sn) or fragmentation occurs before recrystallisation (e.g. Cu-O).

Acknowledgements

This work was supported by EPSRC under grant No. GR/H27250. AMM is grateful to the Royal Society for their support under the University Research Fellowship scheme.

References

1. R. WILLNECKER, D. M. HERLACH and B. FEUERBACHER, *Phys. Rev. Lett.* **62** (1989) 2707.
2. B. T. BASSLER, W. H. HOFMEISTER, G. CARRO and R. J. BAYUZICK, *Metall. Mater. Trans. A* **25** (1994) 1301.
3. R. F. COCHRANE, A. L. GREER, K. ECKLER and D. M. HERLACH, *Mater. Sci. Eng.* **A133** (1991) 698.
4. R. WILLNECKER, D. M. HERLACH and B. FEUERBACHER, in 7th European Symposium on Materials and Fluid Sciences in Microgravity (ESA Special Publication 295, 1989) p. 193.
5. D. LI, T. VOLKMAN, K. ECKLER and D. M. HERLACH, *J. Cryst. Growth* **152** (1995) 101.
6. S. E. BATTERSBY, R. F. COCHRANE and A. M. MULLIS, *Mater. Sci. Eng.* **A226** (1997) 443.
7. D. LI, K. ECKLER and D. M. HERLACH, *J. Cryst. Growth* **160** (1996) 59.
8. S. E. BATTERSBY, R. F. COCHRANE and A. M. MULLIS, *J. Mat. Sci.*, in press.
9. B. L. JONES and G. M. WESTON, *J. Aust. Inst. Met.* **15** (1970) 167.
10. *Idem.*, *ibid.* **15** (1970) 189.
11. R. T. SOUTHIN and G. M. WESTON, *ibid.* **18** (1973) 74.
12. L. A. TARSHIS, J. L. WALKER and J. W. RUTTER, *Metall. Trans.* **2** (1971) 2589.
13. F. GARTNER, A. F. NORMAN, A. L. GREER, A. ZAMBON, E. RAMOUS, K. ECKLER and D. M. HERLACH, *Acta Mater.* **45** (1997) 51.
14. A. J. MCLEOD and L. M. HOGAN, *Met. Trans.* **A9** (1978) 987.
15. J. L. WALKER, in "The Physical Chemistry of Process Metallurgy, Part 2," edited by G. R. St. Pierre (Interscience 1959) p. 845.
16. G. HORVAY, *Int. J. Heat Mass Transf.* **8** (1965) 195.
17. K. KOBAYASHI and L. M. HOGAN, *Met. Forum* **1** (1978) 165.
18. M. SCHWARZ, K. KARMA, K. ECKLER, D. M. HERLACH, *Phys. Rev. Lett.* **73** (1994) 1380.
19. A. M. MULLIS and R. F. COCHRANE, *J. Appl. Phys.* **82** (1997) 3783.
20. D. E. OVSIYENKO, V. V. MASLOV and G. A. ALFINTSEV, *Russ. Met.* (1974) 66.
21. R. F. COCHRANE and D. M. HERLACH, in Proc. VIIth European Symposium on Materials and Fluid Science Under Microgravity, Sept. 1989, Oxford, UK. ESA SP-295, 1989, p. 147.
22. S. P. ELDER and G. J. ABBASCHAIN, in "Principles of Solidification and Materials Processing," edited by R. Trivedi *et al.* (Oxford and IBH Publishing Co. PVT Ltd, Delhi, 1990) p. 299.
23. A. M. MULLIS, *Mater. Sci. and Eng.* **A226** (1997) 804.
24. A. M. MULLIS and R. F. COCHRANE, *J. Appl. Phys.* **84** (1998) 4905.
25. D. MATSON, in Solidification 1998, TMS, Warrendale, PA, ISBN 0-87339-396-1, pp. 233-244.
26. P. K. GALENKO and D. A. DANILOV, *J. Cryst. Growth* **197** (1999) 992.
27. G. L. F. POWELL and L. M. HOGAN, *Trans AIME* **242** (1968) 2133.
28. K. F. KOBAYASHI and P. H. SHINGU, *J. Mater. Sci.* **23** (1988) 2157.
29. M. COSTA AGRO MELLO and C. S. KIMINAMI, *J. Mater. Sci. Lett.* **8** (1989) 1416.
30. S. HENRY, P. JARRY, P. H. JOUNEAU and M. RAPPAZ, *Metall. Mater. Trans.* **A28** (1997) 207.

Received 22 April
and accepted 24 August 1999